Reviewer #2

The study investigates the role of OOM volatility in determining nanoparticle growth rates and demonstrates how uncertainties in volatility parameterizations can affect particle growth predictions. The findings are especially relevant for polluted environments where anthropogenic emissions and NOx chemistry strongly influence OOM composition. The manuscript makes a contribution to understanding the mechanisms controlling NPF and nanoparticle growth. Overall, the manuscript is well written and scientifically sound. I have some minor comments and suggestions below.

Response: We thank *Reviewer #2's* careful evaluation and positive assessment of our work, as well as the constructive comments, which have significantly improved the clarity and quality of our manuscript. Our point-by-point responses are given below.

Comments #1. *"OOMs were generated by hydroxyl radical (OH)-initiated oxidation of toluene or ozonolysis of α-pinene in a Potential Aerosol Mass (PAM) oxidation flow reactor (Aerodyne Research Inc.) operated at a residence time of ~52 s." The OH concentrations employed in PAM reactors are typically much higher than those encountered in the ambient atmosphere. Could the authors discuss how the elevated OH exposure may influence gas-phase oxidation pathways and resulting OOM compositions? To what extent are the OOM yields and molecular compositions measured in this study representative of those formed under atmospheric conditions? A discussion of previous evaluations comparing PAM-generated OOMs with ambient observations would strengthen the atmospheric relevance of the results.*

Response: We thank *Reviewer #2* for this point. We agree that it is central to the atmospheric relevance of our laboratory results. We have added a discussion to Sect. 2.1 (lines 79-90) in our revised manuscript to clearly illustrate the representative of our PAM experiments.

(i) How elevated OH alters the gas-phase pathways.

We agree with *Reviewer #2* that the OH level in the PAM reactor must be stated explicitly. In our toluene experiments, the average [OH] was about 2-6 × 10^9 molecules cm^{-3} (OH exposure of 1.2-3.2 × 10^{11} molecules cm^{-3} s), compared with 0.8-2.4 × 10^7 molecules cm^{-3} at a suburban site in the Yangtze River Delta. Wang et al. (2024) compared the radical budgets of an OFR254 system with those of ambient conditions in Beijing and the Yangtze River Delta and showed that elevated OH shifts the RO_2 fate from autoxidation towards RO_2 + OH, which lowers the fraction of highly oxygenated molecule products. They also showed that, under high-NOx conditions, RO_2 + NO remains the dominant RO_2 pathway as in urban Beijing.

Wang et al. (2024) further examined the product distribution. They found many similarities

between the termination products formed in the reactor and those measured in summertime in urban Beijing, and organonitrates accounted for at least 52% of the monomeric termination products with the presence of NO_x. The reduced contribution from autoxidation reaction pathway at high OH changes the oxygen content of the products, but not their degree of unsaturation, whereas products of secondary OH reactions can be identified by their lower degree of unsaturation. Accretion reactions were also more significant in the reactor than in the ambient atmosphere. The relative abundances of OOMs in our experiments, in particular the shares of highly oxygenated, multi-generation and accretion products, may therefore differ from those in the ambient atmosphere, whereas the types of OOMs formed remain representative of ambient OOMs.

(ii) Previous evaluations of PAM-generated products against chamber and ambient observations.

Several studies have made this comparison directly. Garmash et al. (2020) characterized benzene-derived HOMs in both a flow tube and the JPAC chamber and found the same product families with differences in the relative abundance of species with differing oxygen contents, indicating that the variation of the number of autoxidation steps between different experimental configurations. Cheng et al. (2021) likewise found product distributions are broadly consistent between earlier low-NOx flow tube and chamber studies, while noting that the ambient atmosphere combines much lower OH with much longer reaction times and may therefore favour more oxygenated products from multistep autoxidation. Besides, Palm et al. (2016) confirmed that OFR-derived SOA yields for individual precursors agree with published chamber yields.

Therefore, although the relative abundances or distributions of OOMs slightly differ between the PAM-genartaed and ambient OOMs, their effects on our volatility parameterization could be minor.

We have added the following paragraph at the end of Sect. 2.1 (lines 79-89):

"The ozonolysis of α-pinene experiments were performed under dark condition without UV irradiation, so elevated OH only concerns the toluene + OH experiments. In these experiments, the average OH concentration in the PAM reactor was about 2-6×10^9 molecules cm^{-3} reslting in OH exposure of 1.2-3.2 × 10^{11} molecules cm^{-3} s, and much higher than typical ambient values in the Yangtze River Delta (0.8-2.4 × 10^7 molecules cm^{-3}; Wang et al., 2024). Such conditions favour RO_2 + OH over autoxidation, which may shift the products from highly oxygenated molecules towards less oxygenated and multi-generation species (Peng et al., 2019; Wang et al., 2024). However, under the high-NO_x conditions of our experiments, RO_2 + NO remains the dominant RO_2 pathway, as that in urban Beijing (Wang et al., 2024). Previous

comparisons between flow-reactor, chamber and ambient products also show the same product families, with differences mainly in their relative abundances (Garmash et al., 2020; Cheng et al., 2021). The distribution of OOMs in our experiments may therefore differ from that in the ambient atmosphere, but the types of OOMs formed remain representative of ambient OOMs, which is the basis for our evaluation of the volatility parameterizations."

Comment #2. *"Section 2.3 describes the measurement and quantification of OOMs." Please discuss the limitations and uncertainties associated with the ionization techniques used. Are there classes of OOMs that may be underdetected or missed due to ionization efficiency, molecular structure, volatility, or elemental composition? What fraction of the total OOM population is expected to be detected by the employed instruments? A more comprehensive discussion of measurement biases would aid interpretation of the results.*

Response: We have expanded Sect. 2.3 to discuss these limitations explicitly. Each ionization scheme has its limitation: the nitrate-CIMS requires multiple hydrogen-bond-donating groups for efficient clustering and therefore would underdetects less-oxygenated species and multifunctional carbonyls or esters lacking –OH/–OOH groups; the iodide-CIMS detects polar and acidic species efficiently but discriminates against weakly binding, low-polarity compounds, as quantified by our declustering-voltage scans (Fig. S4); and the Vocus-PTR fragments multifunctional species, in particular peroxides and organic nitrates. The classes most likely to be underdetected are therefore ROOR'-type peroxides, weakly polar multifunctional carbonyls, and sulfur-containing organics.

We instead rely on the complementary coverage of the three instruments: the nitrate-CIMS for highly oxygenated species, the iodide-CIMS for moderately oxygenated and more polar species, and the Vocus-PTR for less oxygenated species, with overlapping detection windows across oxygen numbers and with the quantification rules in Sect. 2.3 applied to species detected by more than one instrument. To the best of our knowledge, this combination covers most of the condensable vapours in our experiments, but we acknowledge that some species, in particular those listed above, may still be missed.

We would also emphasize that incompleteness of OOM detection matters unevenly across the volatility range. The species that control sub-15 nm growth are those of sufficiently low volatility to overcome the Kelvin barrier, and these are highly oxygenated compounds to which the nitrate-CIMS is most sensitive. Undetected compounds are expected to be volatile ones, which cannot contribute to the growth of sub-15 nm particles. Hence, the incompleteness of OOM detection may have no or little effects on our main results.

We have added the following paragraph at the end of Sect. 2.3 (lines 106-116):

"Each of the three ionization schemes carries a characteristic detection bias, and their combination does not amount to a complete coverage of the condensable vapour population. Efficient clustering with NO_3^- requires several hydrogen-bond-donating groups, so that the nitrate-CIMS underdetects less-oxygenated species and multifunctional carbonyls or esters that lack –OH and –OOH functionality. The iodide-CIMS detects polar and acidic species efficiently but discriminates against weakly binding, low-polarity compounds, a bias we quantify through the declustering-voltage scans described above (Fig. S4). The Vocus-PTR fragments multifunctional species, in particular peroxides and organic nitrates, biasing their quantification to the low end. The classes most likely to be underdetected are therefore ROOR'-type peroxides, weakly polar multifunctional carbonyls, and sulfur-containing organics. These biases do not act uniformly across the volatility range. Growth of sub-15 nm particles is controlled by species of sufficiently low volatility to overcome the Kelvin barrier, which are the highly oxygenated compounds to which the nitrate-CIMS is most sensitive, whereas undetected compounds are expected to be volatile ones."

Comment #3. *"Section 2.4 discusses volatility parameterizations and growth simulations." Please elaborate on the uncertainties associated with the applied volatility parameterizations. Specifically, what are the uncertainties in estimated saturation vapor pressures (or C*)?*

Response: We thank the reviewer for this comment. We have added a paragraph to Sect. 2.4 to describe the uncertainties of the volatility parameterizations and how we account for them.

The uncertainty in the estimated C* of an OOM comes mainly from three sources. First, the parameterizations assign a single C* to each molecular formula, whereas isomers of the same formula can differ substantially in functional groups and therefore in their vapour pressure. Second, each scheme is calibrated against a limited set of compounds, specific oxidation systems or measurement conditions, so that its performance outside that domain could be less certain. Third, direct measurements of the volatility of gas-phase OOMs are scarce, and the reference data behind each scheme carry their own uncertainty.

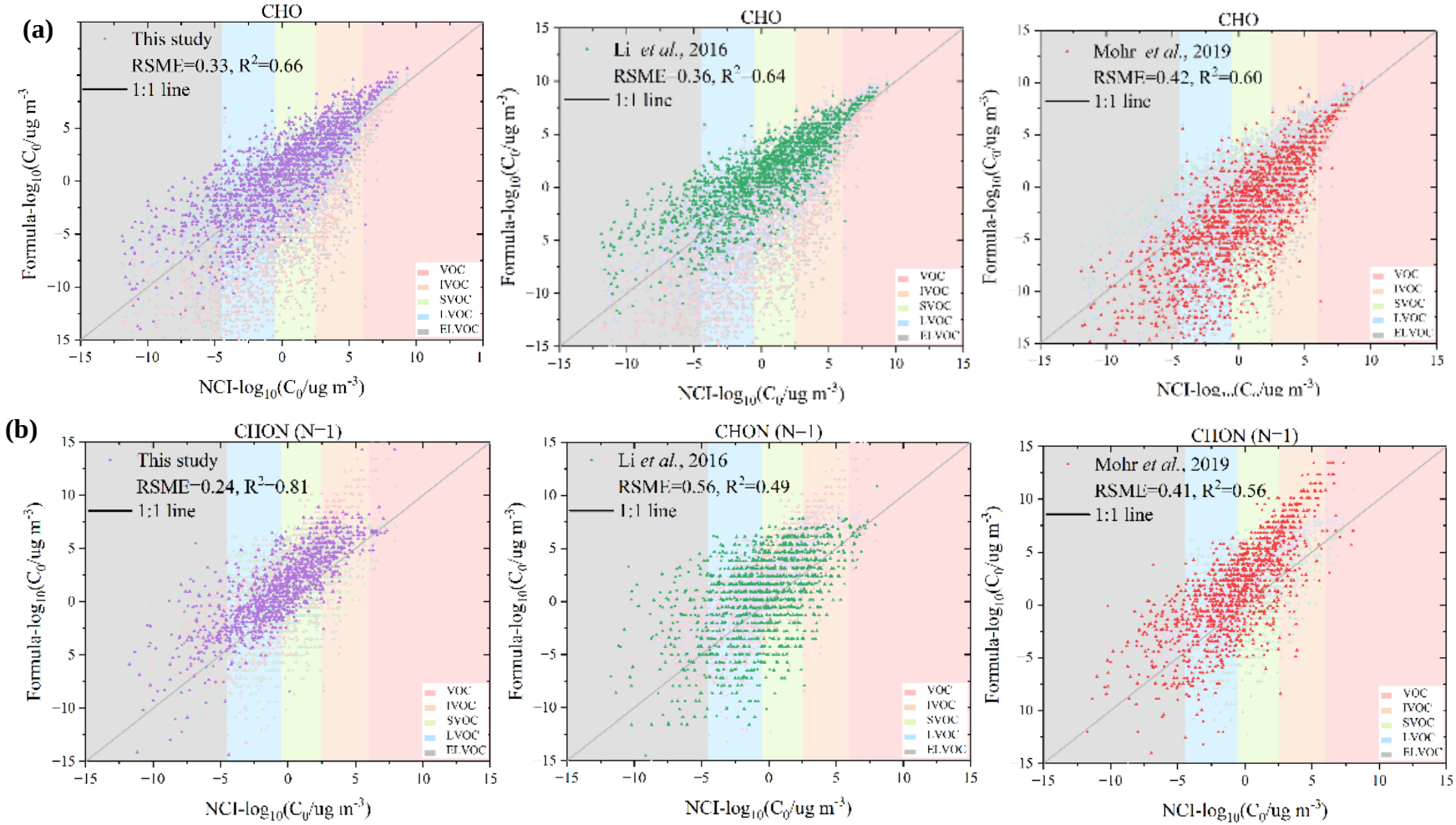
Many of the estimates that enter $\log_{10}$ C* are uncertain, and detailed reference values are lacking. The volatility of compounds with known structures can be estimated, but no direct reference exists for OOMs in the real atmosphere. In the absence of such a reference, a common set of compounds from NCI open database helps to place the schemes relative to one another. Zhang et al. (2026) compared several parameterizations with the NCI open database (1669 CHO, 1243 CHON with one N atom and 639 CHON with two N atoms; $-12 < \log_{10} C^* < 10$), which they chose because it contains many more organic compounds than earlier reference sets and has been used in previous parameterization studies (Fig. R2, reproduced from Fig. S8 of

Zhang et al., 2026). For CHO compounds, the Donahue et al.(2011) and Mohr et al. (2018) schemes deviate visibly from the 1:1 line, whereas the Stolzenburg et al. (2018), Li et al. (2016) and Zhang et al. (2026) schemes agree more closely, with similar R^2 = 0.64, 0.64 and 0.66, respectively. The advantage of Zhang et al. (2026) scheme is obvious for CHON compounds. Its estimates follow the 1:1 line over a wide volatility range (R^2 = 0.81 for one N atom and 0.54 for two N atoms in the formulas), whereas the estimates by Li et al. and Mohr et al. show larger scatter (R^2 = 0.49 and 0.56 for one N; 0.51 and 0.35 for two N). The Mohr et al. estimates also tend to overpredict C_0 for compounds that NCI places at low volatility.

We therefore do not regard any single volatility parameterization as exact, and apply all seven schemes to our laboratory growth experiments. At the same time, the Zhang et al. (2026) scheme is fitted to measured volatilities of a wide range of ambient organic compounds and agrees better with the NCI database, particularly for CHON compounds.

We have added the following paragraph to the revised manuscript (Sect. 2.4, lines 137-142):

"The volatility parameterizations carry uncertainties that should be considered when interpreting the C* values used here. They arise from (i) the assignment of a single C* to each molecular formula, whereas isomers can differ substantially in vapour pressure; (ii) the limited range of compounds and conditions used to calibrate each scheme; (iii) the uncertainty of the reference data, since direct volatility measurements of gas-phase OOMs are scarce. When compared with the NCI open database, the Zhang et al. (2026) scheme performs comparably to the other schemes for CHO compounds and agrees more closely for CHON compounds."


(a)
CHO
This study
RSME=0.33, R²=0.66
1:1 line
Li et al., 2016
RSME=0.36, R²=0.64
1:1 line
Mohr et al., 2019
RSME=0.42, R²=0.60
1:1 line
VOC
IVOC
SVOC
LVOC
ELVOC
Formula-log10(C0/ug m-3)
NCI-log10(C0/ug m-3)
(b)
CHON (N−1)
This study
RSME=0.24, R²=0.81
1:1 line
Li et al., 2016
RSME=0.56, R²=0.49
1:1 line
Mohr et al., 2019
RSME=0.41, R²=0.56
1:1 line

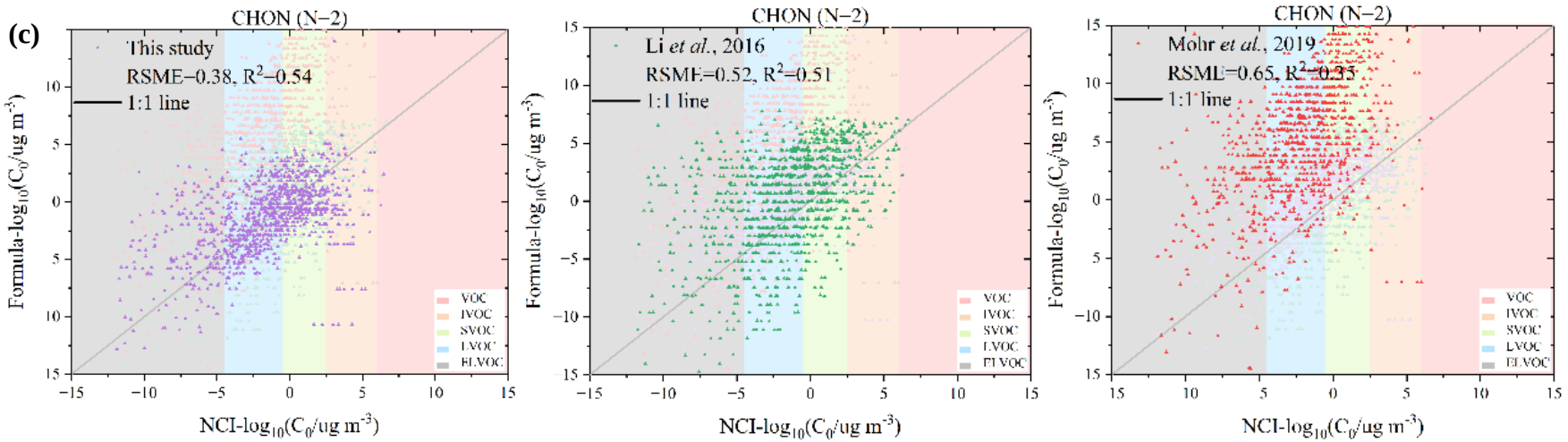


Figure R2. (a) Saturation mass concentrations (C_0) of 1669 CHO compounds estimated by different parametrizations in comparison with the NCI open database. (b) Saturation mass concentrations of 1243 CHON (N=1) compounds estimated by different parametrizations in comparison with the NCI open database. (c) Saturation mass concentrations of 639 CHON (N=2) compounds estimated by different parametrizations in comparison with the NCI open database. The green, red and purple triangles represent Li et al. (2016), Mohr et al. (2019) and Zhang et al. (2026), respectively. The gray, blue, green, orange and red bands represent the regions for ELVOCs, LVOCs, SVOCs, IVOCs and VOCs, respectively. (These figures were cited from the Ref: Zhang et al., 2026)

Comment #4. *On Page 5, "We then simulated nanoparticle growth from the measured saturation vapor pressures and axial concentration profiles of citric acid or PEG-7…" Please clarify whether particle curvature effects on equilibrium vapor pressure were considered once citric acid had condensed into the particle phase. Since Kelvin effects can substantially influence condensation onto nanoparticles in the size range investigated, additional information regarding the treatment of size-dependent vapor pressures in the simulations would be helpful.*

Response: We thank *Reviewer #2* for raising this point. Importantly, the Kelvin effect in our simulations is updated in real time as the particle diameter changes after OOM condensation, rather than being fixed on the diameter of initial seed particles. The growth simulation covers the residence time in our laminar flow reactor with a time step of 1 s, and at every step the equilibrium vapour pressure of each condensing species is recalculated using the particle diameter obtained from the preceding step.

We have added a description of this to Sect. 3.1 (line 182-184).

"The simulation is advanced with a 1 second time step, and at each step the equilibrium vapour pressure of the condensing species is evaluated at the particle diameter reached in the preceding step, so that the curvature-affected equilibrium vapour pressure is tracked continuously as the particle grows."

Comment #5. *On Page 7, "Concentrations of individual OOMs were quantified by instrument-specific calibrations... Note that identical molecular formulas across instruments do not necessarily correspond to identical structures..." Could the authors provide an estimate of the proportion of total gas-phase oxidation products or total OOM mass that was detected and quantified by the instrumentation? Although structural isomers cannot be resolved, it would be useful to understand the extent to which the observed OOM population represents the overall oxidation product distribution.*

Response: We thank the reviewer for this comment. A quantitative carbon closure would be a useful complement, but it is challenging in our experiments. In both systems studied, toluene + OH and a-pinene + O_3, a substantial part of the reacted carbon is expected to be converted to CO, CO_2, formaldehyde and other small volatile products.These species are not OOMs and do not contribute to nanoparticle growth, and they are not quantified by the three CIMS instruments deployed, so the carbon they hold cannot be determined independently. To our knowledge, carbon closure has so far been achieved in only few laboratory oxidation studies (Li et al., 2021; Lambe et al.,2012; Isaacman-VanWertz et al., 2018; Nihill et al., 2023), both of

which relied on multiple complementary instruments. Such a closure investigation is therefore beyond the scope of this study. Besides, a ratio of detected OOM carbon to reacted VOC precursor carbon would therefore reflect mainly how much carbon is converted into these products, rather than how completely the condensable vapours are detected.

Comment #6. *On Page 9, "They are less transferable to polluted, high-NOx environments, where anthropogenic precursors and intensified NOx pathways likely generate OOM populations with distinct functionality, volatility, and condensational behavior." This is an nice conclusion and deserves further discussion. Specifically, how do OOM populations formed under low-NOx and high-NOx conditions differ chemically? Which factors are most responsible for the performance of existing volatility frameworks under low-NOx and high-NOx conditions: molecular functionality, volatility distributions, molecular weight, degree of oxidation, nitrate functionality, or condensational behavior?*

Response: We agree that this point deserves a fuller treatment. Chemically, the two regimes differ through the fate of RO_2. Under low NO_x, RO_2 terminates mainly via $RO_2 + RO_2/HO_2$ in competition with unimolecular autoxidation, yielding CHO products that are highly oxygenated and retain most of the precursor carbon skeleton. Under high NOx, besides $RO_2 + RO_2/HO_2$ reactions, RO_2 + NO dominates and opens two channels that both act to raise volatility: formation of organic nitrates, which appends an $–ONO_2$ group carrying three oxygen atoms; and formation of alkoxy radicals. The mass defect plots in Fig. R3 illustrate this difference. Under high NOx, the region below *m/z* of about 250 is much more densely populated and extends to higher mass defects, consistent with less oxygenated, more fragmented and N-containing species.

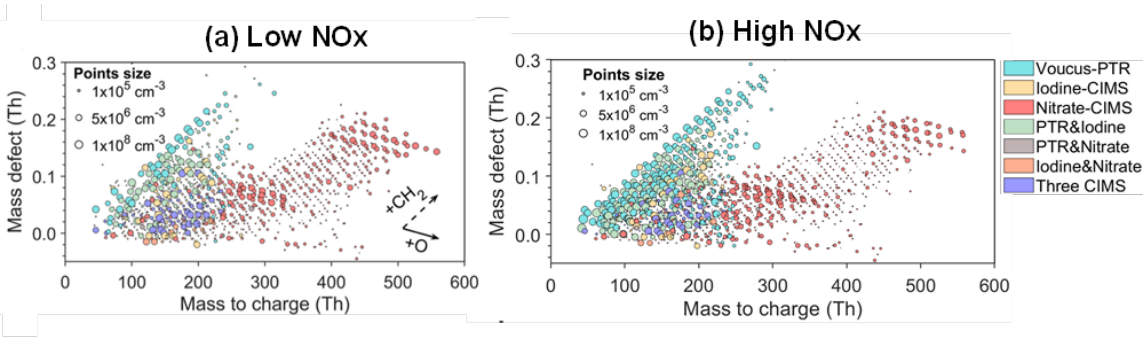


Figure R3. Mass defect plots of all assigned OOMs in the α-pinene + O_3 experiments under (a) low-NO_x and (b) high-NO_x conditions. Marker size scales with OOMs' concentration. Marker color indicates which of the three CIMS (Vocus-PTR, iodide-CIMS, nitrate-CIMS) detected the OOMs, including overlaps, following the color scheme in the bottom right panel.

Of the candidate factors the reviewer lists, nitrate functionality is the dominant one. In every parameterization evaluated here, volatility decreases monotonically with oxygen number; a scheme that does not treat nitrate oxygen separately therefore counts the three oxygens in a –ONO_2 group as if they were hydroxyl or hydroperoxide oxygens, and underestimates $\log_{10}$ C* for each nitrate group. Fragmentation-driven decreases in carbon number act in the same direction but are quantitatively smaller, and the degree of oxidation and molecular weight are largely consequences of these two effects rather than independent causes.

Comment #7. *"In Section 3.3, the authors report the volatility classification of ambient OOMs. One question is whether sulfur-containing OOMs were detected in the ambient measurements. Sulfur-containing organic compounds, including organosulfates and sulfur-containing highly oxidized molecules, may contribute to NPF and nanoparticle growth in polluted environments. If such species were detected, please discuss their abundance and possible role. If not, please clarify whether this reflects their actual absence or limitations of the measurement technique.*

Response: We rechecked our raw mass spectrometry data collected from ambient measurements in Lake Tai for sulfur-containing species. Such species were identified by all three CIMS (253 formulas by Vocus-PTR, 71 by iodide-CIMS and 40 by nitrate-CIMS; Table R2), but they only contributed 2.9%, 5.1% and 1.7% of the respective OOM signals. Most of them were detected by Vocus-PTR and iodide-CIMS, which tend to detect OOMs of relatively high volatility. The Zhang et al. (2026) scheme used in our analysis does not include sulfur element, so it cannot be applied to these species. Applying the Li et al. (2016) scheme, which includes sulfur, indicates that some of the sulfur-containing species could be classified as low-volatility OOMs. However, their signal fraction of total detected OOMs by nitrtate-CIMS was only 1.7%. Therefore, their contribution to the growth of 3-15 nm particles is expected to be minor.

Besides, according to previous studies, the formation of organosulfates mainly occurred in the particle phase, instead of gas phase (Le Breton et al., 2018). However, measuring the chemical composition of sub-15 nm particles remains challenging. Therefore, the potential growth contribution from organosulfates and other sulfur-containing highly oxidized molecules needs further investigations.

Table R2. Sulfur-containing OOMs identified in the Lake Tai measurements by three CIMS, given as the number of assigned molecular formulas and their fractional contribution to the total OOM signal.

	Number of sulfur-containing OOMs	Contribution to total OOM signal (%)
Vocus-PTR	253	2.9
Iodide-CIMS	71	5.1
Nitrate-CIMS	40	1.7

We have made this connection explicit in the revised text (lines 129-130):

"Sulfur-containing OOMs were also detected in the ambient measurements, but because of their low abundance, they were not included in the growth simulations".

References

Cheng, X., Chen, Q., Li, Y. J., Zheng, Y., Liao, K., and Huang, G.: Highly oxygenated organic molecules produced by the oxidation of benzene and toluene in a wide range of OH exposure and NOx conditions, Atmos. Chem. Phys., 21, 12005–12019, https://doi.org/10.5194/acp-21-12005-2021, 2021.

Donahue, N. M., Epstein, S. A., Pandis, S. N., and Robinson, A. L.: A two-dimensional volatility basis set: 1. organic-aerosol mixing thermodynamics, Atmos. Chem. Phys., 11, 3303–3318, https://doi.org/10.5194/acp-11-3303-2011, 2011.

Garmash, O., Rissanen, M. P., Pullinen, I., Schmitt, S., Kausiala, O., Tillmann, R., Zhao, D., Percival, C., Bannan, T. J., Priestley, M., Hallquist, Å. M., Kleist, E., Kiendler-Scharr, A., Hallquist, M., Berndt, T., McFiggans, G., Wildt, J., Mentel, T. F., and Ehn, M.: Multi-generation OH oxidation as a source for highly oxygenated organic molecules from aromatics, Atmos. Chem. Phys., 20, 515–537, https://doi.org/10.5194/acp-20-515-2020, 2020.

Isaacman-VanWertz, G., Massoli, P., O'Brien, R., Lim, C., Franklin, J. P., Moss, J. A., Hunter, J. F., Nowak, J. B., Canagaratna, M. R., Misztal, P. K., Arata, C., Roscioli, J. R., Herndon, S. T., Onasch, T. B., Lambe, A. T., Jayne, J. T., Su, L., Knopf, D. A., Goldstein, A. H., Worsnop, D. R., and Kroll, J. H.: Chemical evolution of atmospheric organic carbon over multiple generations of oxidation, Nat. Chem., 10, 462–468, https://doi.org/10.1038/s41557-018-0002-2, 2018.

Le Breton, M., Wang, Y., Hallquist, Å. M., Pathak, R. K., Zheng, J., Yang, Y., Shang, D., Glasius, M., Bannan, T. J., Liu, Q., Chan, C. K., Percival, C. J., Zhu, W., Lou, S., Topping, D., Wang, Y., Yu, J., Lu, K., Guo, S., Hu, M., and Hallquist, M.: Online gas- and particle-phase measurements of organosulfates, organosulfonates and nitrooxy organosulfates in Beijing utilizing a FIGAERO ToF-CIMS, Atmos. Chem. Phys., 18, 10355–10371, https://doi.org/10.5194/acp-18-10355-2018, 2018.

Lambe, A. T., Onasch, T. B., Croasdale, D. R., Wright, J. P., Martin, A. T., Franklin, J. P., Massoli, P., Kroll, J. H., Canagaratna, M. R., Brune, W. H., Worsnop, D. R., and Davidovits, P.: Transitions from Functionalization to Fragmentation Reactions of Laboratory Secondary Organic Aerosol (SOA) Generated from the OH Oxidation of Alkane Precursors, Environ Sci Technol, 46, 5430-5437, 10.1021/es300274t, 2012.

Li, R., Palm, B. B., Ortega, A. M., Hlywiak, J., Hu, W., Peng, Z., Day, D. A., Knote, C., Brune, W. H., de Gouw, J. A., and Jimenez, J. L.: Modeling the radical chemistry in an oxidation flow reactor: radical formation and recycling, sensitivities, and the OH exposure estimation equation, J. Phys. Chem. A, 119, 4418–4432, https://doi.org/10.1021/jp509534k, 2015.

Li, K., Wentzell, J. J. B., Liu, Q. F., Leithead, A., Moussa, S. G., Wheeler, M. J., Han, C., Lee, P., Li, S. M., and Liggio, J.: Evolution of Atmospheric Total Organic Carbon from Petrochemical Mixtures, Environ Sci Technol, 55, 12841-12851, 10.1021/acs.est.1c02620, 2021.

Li, Y., Pöschl, U., and Shiraiwa, M.: Molecular corridors and parameterizations of volatility in the chemical evolution of organic aerosols, Atmos. Chem. Phys., 16, 3327–3344, https://doi.org/10.5194/acp-16-3327-2016, 2016.

Mohr, C., Thornton, J. A., Heitto, A., Lopez-Hilfiker, F. D., Lutz, A., Riipinen, I., Hong, J., Donahue, N. M., Hallquist, M., Petäjä, T., Kulmala, M., and Yli-Juuti, T.: Molecular identification of organic vapors driving atmospheric nanoparticle growth, Nat. Commun., 10, 4442, https://doi.org/10.1038/s41467-019-12473-2, 2019.

Nihill, K. J., Coggon, M. M., Lim, C. Y., Koss, A. R., Yuan, B., Krechmer, J. E., Sekimoto, K., Jimenez, J. L., de Gouw, J., Cappa, C. D., Heald, C. L., Warneke, C., and Kroll, J. H.: Evolution of organic carbon in the laboratory oxidation of biomass-burning emissions, Atmos. Chem. Phys., 23, 7887–7899, https://doi.org/10.5194/acp-23-7887-2023, 2023.

Peng, Z. and Jimenez, J. L.: Modeling of the chemistry in oxidation flow reactors with high initial NO, Atmos. Chem. Phys., 17, 11991–12010, https://doi.org/10.5194/acp-17-11991-2017, 2017.

Peng, Z., Day, D. A., Ortega, A. M., Palm, B. B., Hu, W., Stark, H., Li, R., Tsigaridis, K., Brune, W. H., and Jimenez, J. L.: Non-OH chemistry in oxidation flow reactors for the study of atmospheric chemistry systematically examined by modeling, Atmos. Chem. Phys., 16, 4283–4305, https://doi.org/10.5194/acp-16-4283-2016, 2016.

Peng, Z., Lee-Taylor, J., Orlando, J. J., Tyndall, G. S., and Jimenez, J. L.: Organic peroxy radical chemistry in oxidation flow reactors and environmental chambers and their atmospheric relevance, Atmos. Chem. Phys., 19, 813–834, https://doi.org/10.5194/acp-19-813-2019, 2019.

Stolzenburg, D., Fischer, L., Vogel, A. L., Heinritzi, M., Schervish, M., Simon, M., Wagner, A. C., Dada, L., Ahonen, L. R., Amorim, A., Baccarini, A., Bauer, P. S., Baumgartner, B., Bergen, A., Bianchi, F., Breitenlechner, M., Brilke, S., Buenrostro Mazon, S., Chen, D., Dias, A., Draper, D. C., Duplissy, J., El Haddad, I., Finkenzeller, H., Frege, C., Fuchs, C., Garmash, O., Gordon, H., He, X., Helm, J., Hofbauer, V., Hoyle, C. R., Kim, C., Kirkby, J., Kontkanen, J., Kürten, A., Lampilahti, J., Lawler, M., Lehtipalo, K., Leiminger, M., Mai, H., Mathot, S., Mentler, B., Molteni, U., Nie, W., Nieminen, T., Nowak, J. B., Ojdanic, A., Onnela, A., Passananti, M., Petäjä, T., Quéléver, L. L. J., Rissanen, M. P., Sarnela, N., Schallhart, S., Tauber, C., Tomé, A., Wagner, R., Wang, M., Weitz, L., Wimmer, D., Xiao, M., Yan, C., Ye, P., Zha, Q., Baltensperger, U., Curtius, J., Dommen, J., Flagan, R. C., Kulmala, M., Smith, J. N., Worsnop, D. R., Hansel, A., Donahue, N. M., and Winkler, P. M.: Rapid growth of organic aerosol nanoparticles over a wide tropospheric temperature range, Proc. Natl. Acad. Sci. USA, 115, 9122–9127, https://doi.org/10.1073/pnas.1807604115, 2018.

Wang, Y., Li, C., Zhang, Y., Li, Y., Yang, G., Yang, X., Wu, Y., Yao, L., Zhang, H., and Wang, L.: Secondary reactions of aromatics-derived oxygenated organic molecules lead to plentiful highly oxygenated organic molecules within an intraday OH exposure, Atmos. Chem. Phys., 24, 7961–7981, https://doi.org/10.5194/acp-24-7961-2024, 2024.

Zhang, X., Li, C., Xue, S., Yang, X., Wang, Y., Li, Y., Cai, R., Yao, L., and Wang, L.: Volatility parametrization of atmospheric organic compounds based on molecular formula, ACS EST Air, 3, 291–301, https://doi.org/10.1021/acsestair.5c00167, 2026.